Conformations of Human Apolipoprotein E(263−286) and E(267−289) in Aqueous Solutions of Sodium Dodecyl Sulfate by CD and ^{1}H NMR[†,‡]

Guangshun Wang,[§] Gregory K. Pierens,[§,||] W. Dale Treleaven,[§,⊥] James T. Sparrow,[#] and Robert J. Cushley*[,§]

Institute of Molecular Biology and Biochemistry, Simon Fraser University, Burnaby, British Columbia V5A 1S6, Canada, and Department of Medicine, Baylor College of Medicine, One Baylor Plaza, Houston, Texas 77030

Received April 17, 1996; Revised Manuscript Received June 6, 1996[⊗]

ABSTRACT: Structures of apoE(263−286) and apoE(267−289) have been determined in aqueous solution containing 90-fold molar excess of perdeuterated sodium dodecyl sulfate by CD and ^{1}H NMR. Conformations were calculated by distance geometry based on 370 and 276 NOE distance restraints, respectively. RMSD for superimposing the region 265−284 from an ensemble of 41 structures for apoE(263−286) is 0.64 ± 0.17 Å for backbone atoms (N, C^α, C═O) and 1.51 ± 0.13 Å for all atoms. The backbone RMSD for an ensemble of 37 structures for apoE(267−289) is 0.74 ± 0.21 Å for the region 268−275 and 0.34 ± 0.10 Å for the region 276−286. A two-domain structure was found for apoE(267−289) with the C-terminal half adopting a very well defined helix and the N-terminal segment 268−275 a less well defined helix, suggesting that the N-terminus may weakly bind to SDS. For apoE(263−286), an amphipathic helix−bend−helix structural motif was found with all hydrophobic side chains on the concave face. The existence of a bend around residues Q273 to G278 is consistent with their temperature coefficients of amide protons as well as secondary shifts of α-protons. Comparison of the structures of the two peptides revealed that the enhanced binding of apoE(263−286) to lipid could be attributed to the formation of a hydrophobic cluster consisting of residues W264, F265, L268, and V269. Aromatic side chains are proposed to be especially important in anchoring apolipoprotein fragments to micelles.

Human serum apoE[1] consists of a single polypeptide chain with 299 amino acid residues (M_r = 34 200) (Rall et al., 1982), which mediates the metabolism of lipids via binding to apoB/E (LDL) receptors (Mahley & Innerarity, 1983). Association with phospholipids is a prerequisite for apoE to bind to the LDL receptor (Innerarity et al., 1979; Weisgraber, 1994).

Thrombin digestion of apoE yields two segments: residues 1−191 and residues 216−299. The N-terminal fragment is purported to contain the receptor-binding domain (Innerarity et al., 1983). The X-ray crystal structure of residues 1−191 shows an antiparallel four-helix bundle (Wilson et al., 1991). The helices, corresponding to residues 24−42, 54−84, 87−122, and 130−164, are all amphipathic and organized with their hydrophobic faces oriented toward the center and their hydrophilic faces directed toward the aqueous phase. The C-terminal thrombolytic fragment is proposed to be the lipoprotein-binding domain (Wetterau et al., 1988) and to be responsible for LCAT activation (Pauw et al., 1995). Truncation mutagenesis studies further defined the lipid binding domain to residues 267−299 (Westerlund & Weisgraber, 1993). Using synthetic apoE peptides, Sparrow et al. (1992) found that segment 267−286 did not associate with DMPC while 263−286 did. Segment 263−286 has thus been proposed as one of the primary lipid-binding regions of apoE (Sparrow et al., 1992; Pauw et al., 1995).

Micelles of SDS or dodecylphosphocholine (DPC) have been widely utilized to investigate conformations of membrane proteins or peptides (Brown & Wüthrich, 1981; Wüthrich, 1986; Inagaki et al., 1989; McDonnell & Opella, 1993; Rizo et al., 1993; Henry & Sykes, 1994). Recently, we have shown that both SDS and DPC can be used to model the lipid environments of lipoproteins (Rozek et al., 1995; Buchko et al., 1996; Wang et al., 1996). In order to elucidate the structural details of apoE(263−286) and apoE(267−289) bound to lipid, we have performed fluorescence and CD spectroscopy and 2D NMR studies of both peptides in the presence of SDS micelles. Here, we report the results of these studies.

MATERIALS AND METHODS

ApoE(267−289), PLVEDMQRQWAGLVEKVQAAVGT, was purchased from Dr. Ian Clark-Lewis (University of

[†] This work was supported by the Natural Sciences and Engineering Research Council of Canada.

[‡] Brookhaven Protein Data Bank identification numbers: 1OEF (coordinates) and R1OEFMR (restraints) for apoE(263−286); 1OEG (coordinates) and R1OEGMR (restraints) for apoE(267−289).

* Address correspondence to this author.

[§] Simon Fraser University.

[||] Present address: Faculty of Science and Technology, Griffith University, Nathan Campus, Kessels Road, Brisbane QLD 4111, Australia.

[⊥] Present address: College of Basic Science, Louisiana State University, Baton Rouge, LA 70803.

[#] Baylor College of Medicine.

[⊗] Abstract published in *Advance ACS Abstracts,* July 15, 1996.

[1] Abbreviations: apoE, apolipoprotein E; LDL, low density lipoproteins; apoB, apolipolipoprotein B; apoA-I, apolipoprotein A-I; LCAT, lecithin:cholesterol acyltransferase; DMPC, dimyristoylphosphatidylcholine; SDS, sodium dodecyl sulfate; DPC, dodecylphosphocholine; *t*-Boc, *tert*-butoxycarbonyl; HF, hydrogen fluoride; TFA, trifluoroacetic acid; FAB, fast atom bombardment; CD, circular dichroism; NOESY, nuclear Overhauser enhancement spectroscopy; TOCSY, total correlation spectroscopy; DQF-COSY, double-quantum-filtered correlation spectroscopy; RMSD, root mean square deviation; ppb/K, ppm × 10^{-3}/deg.

S0006-2960(96)00934-8 CCC: $12.00

British Columbia, BC, Canada). Perdeuterated sodium dodecyl sulfate (SDS-d_{25}, 98% D) was purchased from Cambridge Isotope Laboratories (MA, USA), SDS from BDH Chemical Ltd. (Poole, England), and deuterium oxide (99.9% D) from Isotec Inc. (OH, USA).

Synthesis and Purification of ApoE(263−286). ApoE-(263−286), SWFEPLVEDMQRQWAGLVEKVQAA, was synthesized on an Applied Biosystems 430A synthesizer using Boc chemistry starting with BocAla-PAM resin obtained from ABI. The synthesis programs were minor modifications of the programs supplied with the instrument. As the last step of the synthesis, the formyl group was removed from Trp by treatment with piperidine/DMF prior to deprotection of the Boc group and drying of the resin. The resin was placed in a vacuum desiccator overnight prior to cleavage and deprotection with HF. The peptide was cleaved from the resin by treatment of 1 g of resin with 30 mL of anhydrous HF containing 3 mL of anisole and 0.3 mL of ethanedithiol at −20 °C for 3 h. The HF was removed under vacuum, and the peptide and resin were precipitated and washed with ether. The peptide was dissolved with TFA and the resin removed by filtration. The TFA was evaporated with a rotary evaporator connected to a vacuum pump and the peptide again precipitated with ether. The peptide was collected by centrifugation and dissolved in 1 M Tris/6 M guanidine hydrochloride and desalted on a 5 × 50 cm column of Bio-Gel P-2 equilibrated with 0.1 M ammonium bicarbonate. The peptide-containing fractions were lyophilized. The crude peptide was purified by reversed-phase HPLC on a 2.2 × 25 cm Vydac 214TP101522 column equilibrated in 0.1% TFA at a flow rate of 20 mL/min and eluted with a 1 h gradient from 15% to 40% 2-propanal, 0.1% TFA. The peptide-containing fractions were lyophilized, and the peptide was dissolved in water. The peptide was judged pure by analytical HPLC and had the expected amino acid composition and sequence. A mass of 2819 was found by FAB mass spectroscopy; expected mass was 2818.2.

Circular Dichroism. CD spectra were recorded on a Jasco J710 spectropolarimeter calibrated using *d*-(+)-camphorsulfonate. Temperature was regulated with a Neslab RTE-110 circulating water bath to 25.0 ± 0.5 °C. The pH (±0.1) of the sample was measured by inserting a glass electrode into the CD cell. Two scans were collected from 190 to 260 nm for each sample, using a 0.1 cm path length cell, with a band width of 0.5 nm, scan speed of 20 nm per minute, and reponse time of 0.25 s. After background subtraction and smoothing, spectra were converted to molar elipticity per residue in deg cm^{-2} $dmol^{-1}$. The peptide concentration was determined by the method of Lowry et al. (1951) using bovine serum albumin as standard. The CD data from 195 to 240 nm were analyzed using convex constraint analysis to generate pure components corresponding to different secondary structures (Perczel et al., 1992).

Nuclear Magnetic Resonance. Solutions of apoE(267−289) (2.9 mM) or apoE(263−286) (5 mM) in the presence of SDS-d_{25} (peptide/SDS 1:90, mol/mol) were prepared in 0.6 mL of 90% H_2O and 10% D_2O. The pH (meter reading without isotope effect correction) of the sample was measured directly in the 5 mm NMR tube and adjusted using NaOH or HCl.

TOCSY (Braunschweiler et al., 1983; Bax & Davis, 1985), NOESY (Jeener et al., 1979), and DQF-COSY (Rance et al., 1983) spectra were acquired at a ^{1}H resonance frequency of 600.13 MHz on a Bruker AMX 600 spectrometer in the phase-sensitive mode using time-proportional phase incrementation (TPPI) (Redfield & Kuntz, 1975). Typically, spectra were collected with 2K data points in t_2, 640 increments (32 scans each) in t_1, and a spectral width of 7246.4 Hz in both dimensions. The water signal was suppressed by the WATERGATE technique (Piotto et al., 1992) using a 3-9-19 pulse sequence (Sklenár et al., 1993) for TOCSY and NOESY experiments. In the DQF-COSY experiments, the water signal was suppressed by presaturation during the recycling delay. NOESY experiments were collected at mixing times of 50, 75, 100, 150, and 225 ms. TOCSY experiments were performed at a mixing time of 75 or 100 ms with a 2.5 ms trim pulse at the end of the MLEV-17 spin-locking sequence. NMR data were apodized by a 90°-shifted sine-bell window function in F_2 and 0° in F_1 for spectra of apoE(263−286) and 60°-shifted sine-bell window function in both dimensions for spectra of apoE-(267−289), zero-filled, and Fourier transformed on a Silicon Graphics workstation using FELIX 2.30 (Biosym Technologies, Inc.) to give a matrix of 2K × 2K. Baselines were corrected using a fifth order polynomial function in both dimensions. Chemical shifts were referenced to sodium 2,2-dimethyl-2-silapentane-5-sulfonate (DSS, 0.00 ppm).

To measure temperature coefficients for amide protons, NOESY (mixing time 100 ms) and TOCSY spectra were collected with 2K data points in t_2 and 400 increments (16 scans each) in t_1 under the same conditions as above from 22 to 47 °C in steps of 5 °C.

Structure Calculations. Three-dimensional structures of the peptides in SDS-d_{25} micelles were calculated from the NOE volumes (FELIX) using the distance geometry program DGII of Insight II (Biosym Technologies) (Havel, 1991) as described by Rozek *et al.* (1995) except (1) the initial distance restraints used to calculate structures were obtained by classifying the peak volumes into strong (1.8−2.8 Å), medium (1.8−3.8 Å), and weak (1.8−5.0 Å) ranges (Gronenborn & Clore, 1995) as opposed to ranges of 1.8−2.5, 2.5−3.5, and 3.5−5.0 Å, (2) an extended covalent peptide structure with *trans* peptide bonds was used as starting structure, and (3) consistent valence force field upper and lower force constants were set at 10 kcal mol^{-1} $Å^{-2}$ for apoE-(263−286) and 32 kcal mol^{-1} $Å^{-2}$ for apoE(267−289) calculations with a maximum force constant of 100 kcal mol^{-1} $Å^{-2}$ for both.

RESULTS

Figure 1 depicts the CD spectra of apoE(263−286) (A) and apoE(267−289) (B). In the absence of SDS, both peptides are dominated by random structure as indicated by the strong negative band at 198−200 nm (Woody, 1995). Convex constraint analysis (Perczel et al., 1992) yields 68% and 62% random coil, 21% and 27% β-structure, and 7% and 2% α-helix, for apoE(263−286) and apoE(267−289), respectively. The significant amount of β-structure found for lipid-associating, amphipathic peptides in the absence of lipids has been reported earlier and was attributed to peptide aggregation via intermolecular β-sheets, forming to protect the large hydrophobic face (Zhong et al., 1994). Addition of SDS induced a dramatic change in the spectra of both peptides. At a peptide/SDS molar ratio of 1:5 or greater, the CD spectra for both peptides are characterized by a

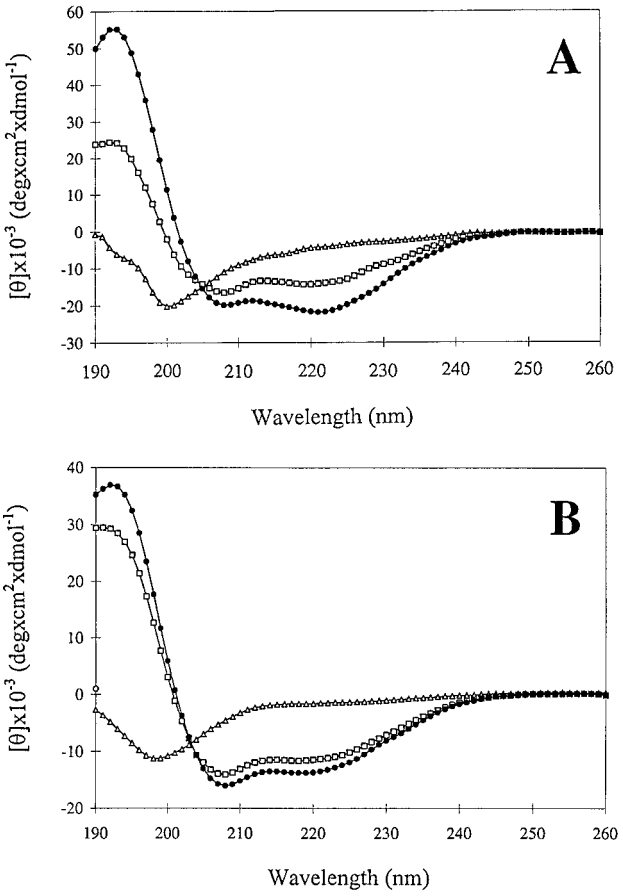

FIGURE 1: CD spectra of 0.10 mM apoE(263−286) (A) and apoE(267−289) (B) in water and in the presence of different concentrations of SDS: (△) no SDS; (□) 0.5 mM SDS; and (●) 9 mM SDS at 25 °C, pH 5−6.

positive band at 192−193 nm and double minima at 208 and 222 nm (Figure 1), features which are characteristic of helical structure (Holzwarth & Doty, 1965; Woody, 1995). The figure suggests that all of the peptide was bound to SDS in a micelle-bound state (Bairaktari et al., 1990) at peptide/SDS molar ratios of 1:90, where there was 67% and 51% α-helix estimated by convex constraint analysis of the CD spectra for apoE(263−286) and apoE(267−289), respectively, indicating a longer helical segment in the former.

At saturating levels of SDS a 19 nm blue-shift of the Trp fluorescence of both peptides was measured (figures not shown). Such a shift in the Trp fluoresence is due to transferring the aromatic ring(s) from an aqueous to a hydrophobic environment (Sparrow et al., 1992; Mishra et al., 1994) and indicates an association of peptide with SDS micelles. The helix content (67%) and the magnitude of the Trp fluorescence blue-shift for apoE(263−286) are similar to values obtained in DMPC (Sparrow et al., 1992).

Resonance Assignments and Secondary Shifts. NMR signals of apoE(267−289) were found to shift considerably at peptide/SDS molar ratios of 1:5 or higher, indicating a change in conformation in SDS. At SDS molar ratios of 5-fold or lower the lines were broad due to exchange between free peptide and peptide bound to SDS micelles. However, at a peptide/SDS ratio of 1:90 a single set of well resolved, sharper signals was found with line widths approximately 10 Hz. This is consistent with all of the peptide binding to a micellar complex (Lauterwein et al., 1979; McDonnell & Opella, 1993; Henry & Sykes, 1994). Best resolution of H^N signals in the presence of SDS was obtained at pH 4.8 for apoE(263−286) and pH 6.0 for apoE(267−289). For both peptides no evidence was found for conformational change from pH 4 to 7.

All 2D NMR spectra were assigned to one set of signals using standard procedures (Wüthrich, 1986). Figure 2A shows portions of the NOESY spectrum of apoE(263−286) in SDS-d_{25}. TOCSY was used to identify spin systems, and NOESY was used for sequential assignments. The complete assignment of longer side chains was confirmed by DQF-COSY. At 37 °C, the H^N signal of W264 was very weak, the assignment of which was confirmed by NOESY at 27 °C. Also, at the lower temperature H^N and H^δ of F265 and H^α of W276 were completely resolved. The spectra of apoE(267−289) (Figure 2B) in SDS were assigned similarly. Because of the overlap of H^N signals for M272 and W276, their side chain connectivities were corroborated by comparison with the NOESY spectra at 27 °C. Tables of chemical shifts are included in the Supporting Information.

From H^α secondary shifts for apoE(267−289) the region V268 to A286 is most likely helical whereas for apoE(263−286) the region S263 to Q284 appears to be a helical structure. The H^α secondary shift is the difference between the H^α chemical shift in a random coil (Wüthrich, 1986) and the measured shift. A grouping of secondary shifts greater than 0.1 ppm is indicative of a helical structure (Wishart et al., 1991, 1992). For both peptides secondary shifts for most of the residues in the region Q275−G278 are close to zero, suggesting the structure around that region is less ordered (Wishart et al., 1992; Chupin et al., 1995). Based on the secondary shifts, the helix content can be estimated using the average secondary shift per residue divided by 0.35, a value where 100% helix is assumed (Rizo et al., 1993). The amount of helix obtained is 60% for apoE(263−286) and 58% for apoE(267−289). These percentages are similar to those found by CD for the two peptides.

Temperature Dependence of Amide Proton Signals. Temperature coefficients for H^N signals of apoE(263−286) and apoE(267−289) in SDS micelles are presented in Figure 3. Temperature coefficients have been used as evidence for hydrogen bonds or solvent accessibility and to determine the secondary structures in peptides (Basu et al., 1991; Raj et al., 1994; Yee et al., 1995). Temperature coefficients ranging from −3.0 to 0 ppb/K have been regarded as hydrogen-bonded, −3 to −4.5 ppb/K as weakly hydrogen-bonded, and −5 to −12 ppb/K as solvent-exposed (Yee et al., 1995). In apoE(263−286) amide protons of residues W264, E266, L268, D271, G278, E281, K282, A285, and A286 are suggested to be hydrogen-bonded, whereas for apoE(267−289) amide protons of residues D271, G278, E281, K282, A286, and G288 may be hydrogen-bonded. While hydrogen bonds were found along the entire sequence of apoE(263−286), in apoE(267−289) most were located at the C-terminus, indicating the N-terminus of that peptide is less ordered. In both peptides, the backbone amide protons of residues 272−277 are most sensitive to temperature, indicating the region is highly solvent accessible.

Secondary Structure. Figure 4A is a summary of interresidue NOEs of apoE(263−286) in the presence of SDS-d_{25}. Medium to strong H^N_i−H^N_{i+1}, H^α_i−H^N_{i+1}, H^α_i−H^N_{i+3}, and H^α_i−H^β_{i+3} and weak to medium H^α_i−H^N_{i+4}, H^α_i−H^N_{i+2}, and H^N_i−H^N_{i+2} NOE connectivities were found for the region L266−A286, indicating an α-helix structure (Wüthrich,

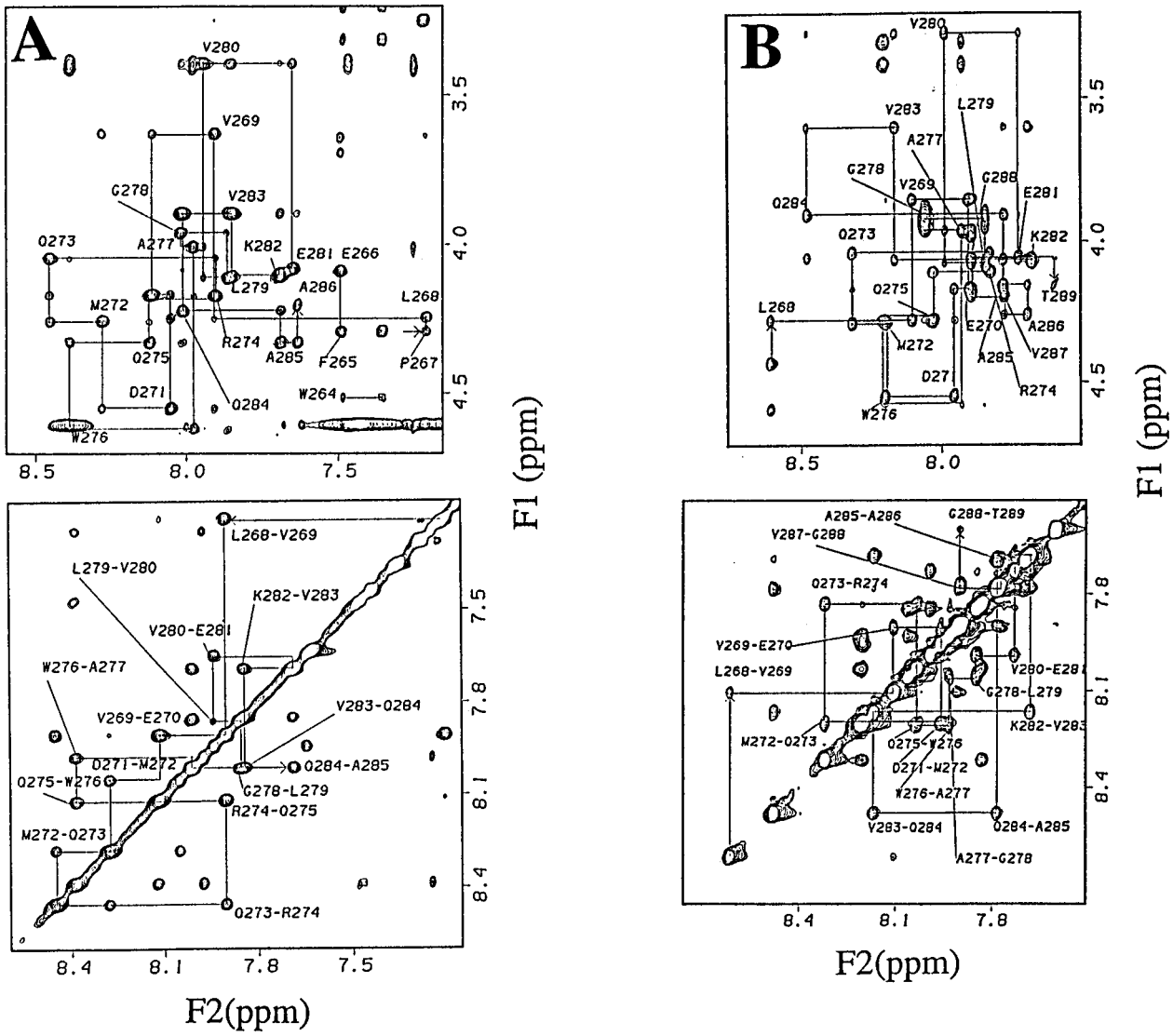

FIGURE 2: NOESY (mixing time 150 ms) fingerprint (top) and amide regions (bottom) of (A) 5 mM apoE(263−286) in the presence of 450 mM SDS-d_{25} (peptide/SDS 1:90 mol/mol) at pH 4.8 and 37 °C and (B) 2.9 mM apoE(267−289) in the presence of 261 mM SDS-d_{25} (peptide/SDS 1:90 mol/mol) at pH 6.0 and 37 °C. The constructs follow the sequential NOE connectivities with H^{α} peaks in the fingerprint region and H^N-H^N cross peaks in the amide region labeled.

1986). In addition, the N-terminus contains many ($i-i+3$) and ($i-i+4$) NOE connectivities between aromatic rings of W264 or F265 and the side chains of L268 or V269, suggesting the helical structure extends to W264. NOE cross peaks between P267 H^{δ} and E266 H^N, as well as P267 H^{δ} and E266 H^{α}, but not between P267 H^{α} and E266 H^{α} indicate the E266−P267 peptide bond is predominantly in the *trans* conformation (Wüthrich, 1984). Inclusion of a proline in a helical region has been reported for several peptides (Barlow & Thornton, 1988; Yun et al., 1991; Yuan et al., 1995; Johnson et al., 1994).

Interresidue NOEs for apoE(267−289) in SDS are summarized in Figure 4B. NOE connectivities support an α-helix structure for the region 277−288. A combination of strong $H^{\alpha}_i-H^N_{i+1}$, weak $H^{\alpha}_i-H^N_{i+2}$, $H^{\alpha}_i-H^N_{i+3}$, and $H^N_i-H^N_{i+2}$, and weak to medium $H^{\alpha}_i-H^{\beta}_{i+3}$ NOEs for residues 267−276 of apoE(267−289), as well as strong TOCSY relayed peaks from amide protons to side chains, suggests an unstable helical structure (Buchko et al., 1995; Dyson et al., 1988, 1992). Therefore, the N-terminus of apoE(267−289) is probably weakly bound to SDS (Pierens et al., 1995).

Three-Dimensional Structures of ApoE(263−286) and ApoE(267−289) in SDS-d_{25}. For the final DGII calculation, 370 NOE distance restraints (194 interresidue and 176 intraresidue) for apoE(263−286) and 276 NOE restraints (143 interresidue and 133 intraresidue) for apoE(267−289) were used. Figure 5A shows an ensemble of 41 structures of apoE(263−286) and Figure 5B 37 structures of apoE-(267−289), where the backbone atoms (N−C^{α}−C═O) have been superimposed. From the ensemble, the RMSD for superimposing residues 265−284 of apoE(263−286) to the average structure is 0.64 ± 0.17Å for backbone atoms and 1.51 ± 0.13 Å for all atoms. The backbone RMSD of apoE-(267−289) is 0.75 ± 0.21 Å for residues 268−275 and 0.34 ± 0.10 Å for residues 276−286, respectively.

Figure 6 is a plot of pairwise RMSD versus residue position. The RMSD for superimposition of all atoms for both peptides is generally below 1.5 Å. Increased backbone RMSD values for the termini of the two peptides indicates fraying of the ends (Shoemaker et al., 1987). Backbone atoms in the N-terminus of apoE(267−289), e.g., from residues 270 to 282, are less well defined than those at the

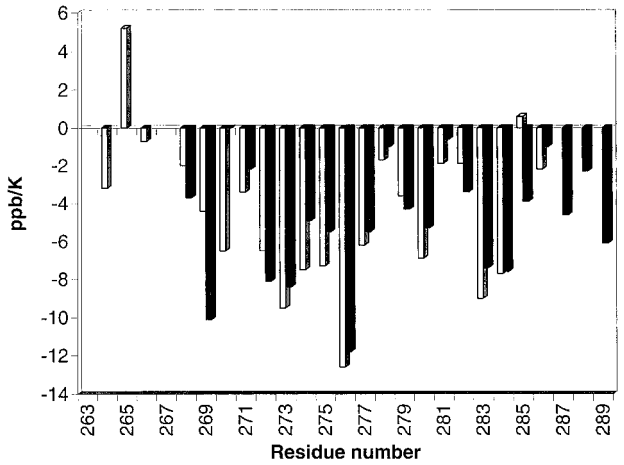

FIGURE 3: Plots of temperature coefficients of amide protons of apoE(263−286) (white column) and apoE(267−289) (black column) in SDS-d_{25} versus residue number. Temperature coefficients are slopes obtained from linear least-squares fits of the H^N chemical shifts versus temperature. Chemical shifts, referenced to internal DSS, were obtained from NOESY spectra at a mixing time of 100 ms.

C-terminus, and the N-terminus of apoE(263−286) is better defined than that of apoE(267−289). This is evident in the superimposed structures (Figure 5). For apoE(263−286) the RMSD of all atoms for residues Q273−Q275 are as large as those of terminal residues (Figure 6A), supporting our contention that this part of the helix is less well defined.

A stereoview of side chain orientations is shown in Figure 7, from which the hydrophobic (medium gray), hydrophilic (light gray), and interfacial (dark) faces can be seen. Side chains, especially hydrophilic ones, are less well defined than backbone atoms due to fewer interresidue restraints and quenching of NOEs by side-chain mobility (Berndt et al., 1996). For clarity, we show in Figure 8 the average orientation for side chains of apoE(263−286) (8A) and apoE-(267−289) (8B) with the backbone atoms replaced by ribbons. For apoE(263−286), an amphipathic helix−bend−helix structural motif was found with a bend angle of approximately 150° (Figure 8A). This bend around residues 273−278, evident in Figures 5A and 7A, is consistent with H^α secondary shifts as well as temperature coefficients (Figure 3). A similar structural motif was reported for melittin bound to DPC micelles (Inagaki et al., 1989) and a signal peptide (Chupin et al., 1995). All hydrophobic side chains in apoE(263−286) are clustered on the concave face and E266, P267, E270, R274, E281, and A283 on the convex hydrophilic face. Residues D271, Q273, Q275, A277, K282, and Q284 are found at the interface. These same interfacial residues are oriented similarly in the structure of apoE(267−289) (Figures 7B and 8B).

As shown in Figure 8, the aromatic side chain of W276 in the average structures of both peptides forms a 35−50° angle with the helix long axis and lies close to V280. As a result, the chemical shifts of H^α, H^β, and one of the H^γ of V280 are ring current shifted to higher field (Johnson & Bovey, 1958) compared to other valines. The ring current effect between residue *i* (W276) and *i*+4 (V280) further supports a helical structure for that part of the molecule. In apoE(263−286), (Figure 8A), F265 forms an 85° angle with the helix long axis. In addition, W264 lies close to L268 and F265 in apoE(263−286). This accounts for the upfield shifts of H^N, H^β, H^δ of F265, and H^N of L268. The slightly different orientation of W276 rings in the two peptide structures may explain the difference in the secondary shift of V280.

DISCUSSION

The segment apoE(268−285) has been classified as a class G* amphipathic helix based on the helical wheel projection (Segrest et al., 1990, 1994). A G* helix is similar to, but not identical with, an α-helix found in globular proteins. It has charged and polar residues randomly distributed on the hydrophilic face. The distribution of charged and polar side chains around the helix long axis, as shown in the structures determined from NMR restraints (Figures 7 and 8), indicates that both apoE(263−286) and apoE(267−289) can be classified as a G* amphipathic helix. There are some important differences from an "ideal" helix as depicted in a helical wheel projection, however. For example, in apoE-(267−289) V269 is not found on the hydrophobic face (Figure 8B). Also, apoE(263−286) does not adopt an ideal long helix in SDS as depicted by the helical wheel, but rather a helix−bend−helix motif. Based on primary sequence

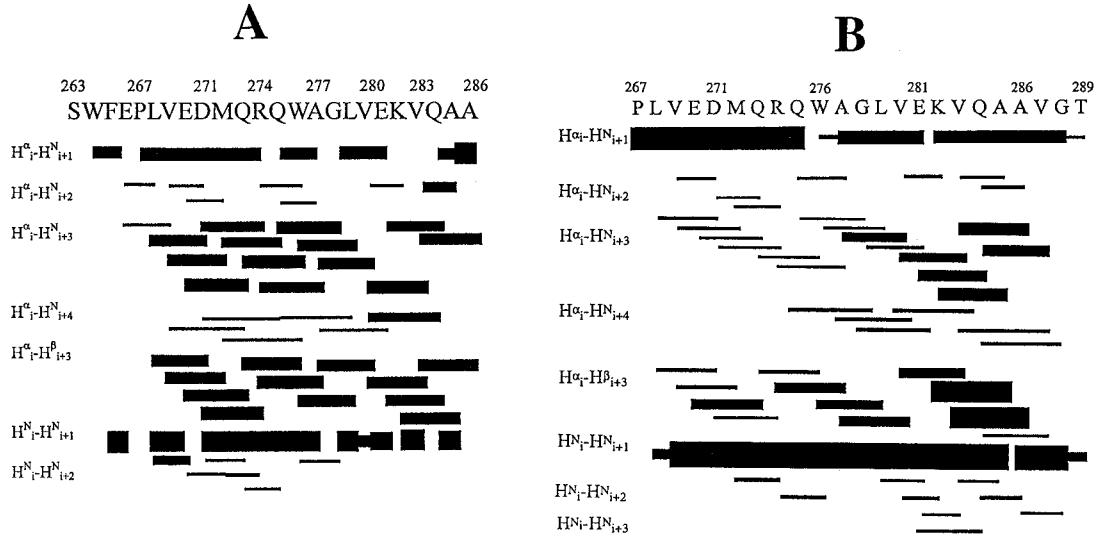

FIGURE 4: Summary of interresidue NOEs observed for apoE(267−289) (A) and apoE(267−289) (B) in an aqueous solution of SDS-d_{25} (peptide/SDS ratio 1:90 mol/mol) at a mixing time of 100−150 ms. NOE intensities are indicated by the height of the bar.

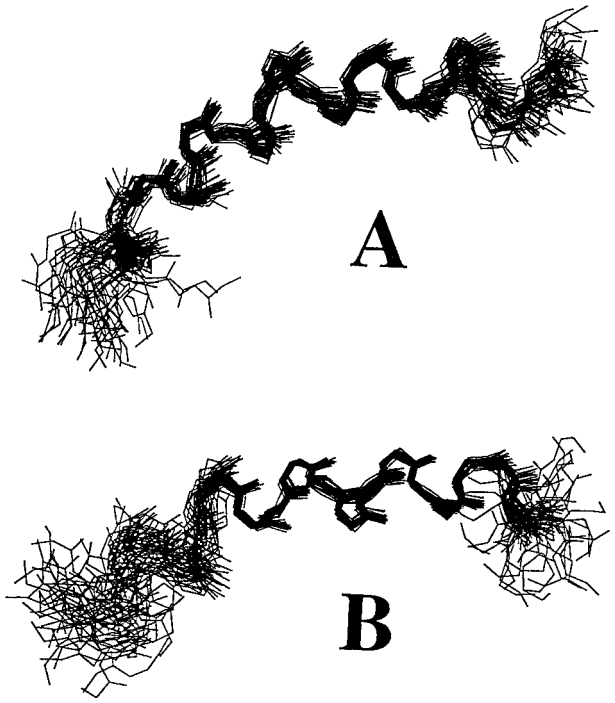

FIGURE 5: Superimposed backbone view of an ensemble of 41 structures out of 50 for apoE(263−286) (A) and an ensemble of 37 structures out of 50 for apoE(267−289) (B) calculated by DGII as decribed in Materials and Methods using NOE restraints derived from NOESY spectra of the peptides bound to SDS-d_{25}. The backbone atoms (N−C$^{\alpha}$−C═O) of residues E266−Q284 for apoE-(263−286) and residues Q275−Q284 for apoE(267−289) have been superimposed.

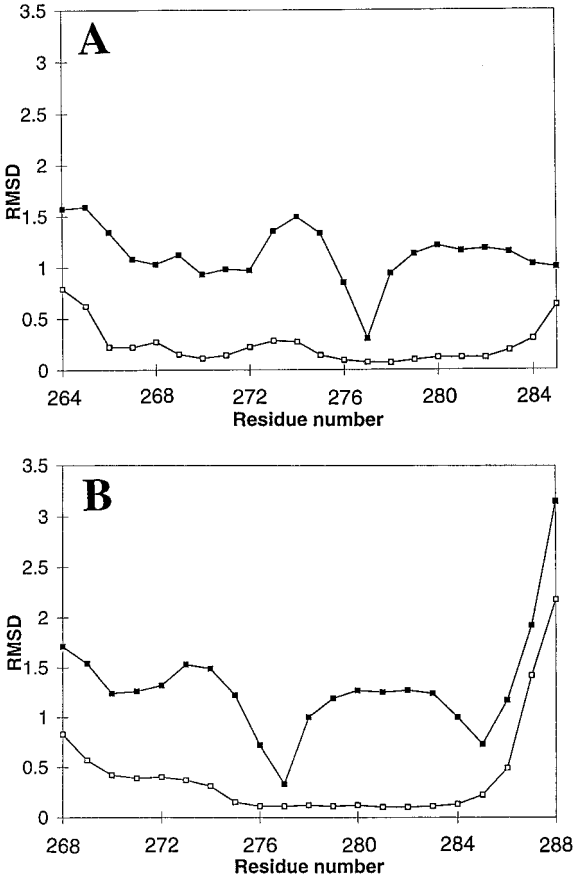

FIGURE 6: Plots of pairwise RMSDs (Å) to the mean structure for superimposition of all atoms (solid squares) and backbone atoms N−C$^{\alpha}$−C═O (open squares) for each residue of apoE(263−286) (A) and apoE(267−289) (B). Data were smoothed using a three-residue window.

prediction algorithms and CD data, Nolte and Atkinson (1992) have proposed a helix from residues 264−271, a β-structure from 273−277 and a helix from 279−285. While we see no evidence of β-structure, neither pleat nor turn, the bend we find in the vicinity of residues 273−278 corresponds exactly with Nolte and Atkinson's proposed β region.

Recently, we have shown that, in apoA-I(166−185), a class A amphipathic helix, all three interfacial arginines interact with SDS micelles (Wang et al., 1996). In both apoE peptides, as shown in Figures 7 and 8, only one cationic side chain, K282, is found in the interface. Therefore, electrostatic interaction between negatively charged SDS head groups and positively charged peptide side chains does not appear to be essential in the binding of the peptides to the micelle. Instead, they bind to lipid predominantly by exposing a large hydrophobic surface. This supports our previous proposal that hydrophobic interactions are the major contributor to stabilizing the lipid−peptide complex (Rozek et al., 1995; Buchko et al., 1996).

On the basis of transfer free energies for amino acids, Brasseur et al. (1992) have calculated the atomic transfer energy values (δG_i) for seven different hybridization states of atoms in peptide residues. Assuming that side chain transfer energy from aqueous phase to SDS micelles is the sum of the atomic transfer energy, the hydrophobic binding free energy (ΔG_{hb}) for an amphipathic helix can be estimated by summing the transfer free energy of all hydrophobic side chains. From the residues found in the hydrophobic faces of the calculated structures (Figures 7 and 8) the ΔG_{hb} was calculated to be −123 kcal/mol for apoE(263−286) and −92 kcal/mol for apoE(267−289). Since the fragments are of similar length (24 versus 23 residues), we attribute the more favorable ΔG_{hb} for apoE(263−286) to the additional pair of aromatic residues, W264 and F265. This may explain, in part, why apoE(263−286) binds to DMPC and apoE(267−286) ($\Delta G_{hb} = -81$ kcal/mol) does not (Sparrow et al., 1992).

In proteins, aromatic rings on adjacent residues are frequently oriented perpendicular to one another, approximately 4.5−7 Å apart. This is believed to result from favorable partial charge interaction between hydrogen atoms on the edge of one ring and carbon atoms on the face of the other ring (Burley & Petsko, 1985; Serrano et al., 1991). As can be seen in Figure 8A, the aromatic rings of W264 and F265 in the average structure are oriented more or less perpendicular to one another. The distances between aromatic H$^{\delta}$ or H$^{\epsilon}$ protons of F265 and the carbons of the six-membered ring of W264 are 4−6 Å. A ring current shift of 0.5 ppm is observed for H$^{\delta}$ of F265. A large upfield shift of H^{N} for L268 (1.42 ppm) is also observed. Taken together with the NOEs found between side chains of W264, F265, L268, and V269, a hydrophobic cluster of these four residues is proposed. While aromatic−aromatic interactions (−1 to −2 kcal/mol) have been found to stabilize protein tertiary and quaternary structures (Burley & Petsko, 1985; Serrano et al., 1991), we propose that the WFLV hydrophobic cluster, including the WF aromatic pair, plays an important role in the stabilization of the amphipathic helix structure at the N-terminus of apoE(263−286) by intercalation of aromatic side chains into the hydrophobic core of the SDS micelle (Figure 5A). A similar N-terminus stabilization has been

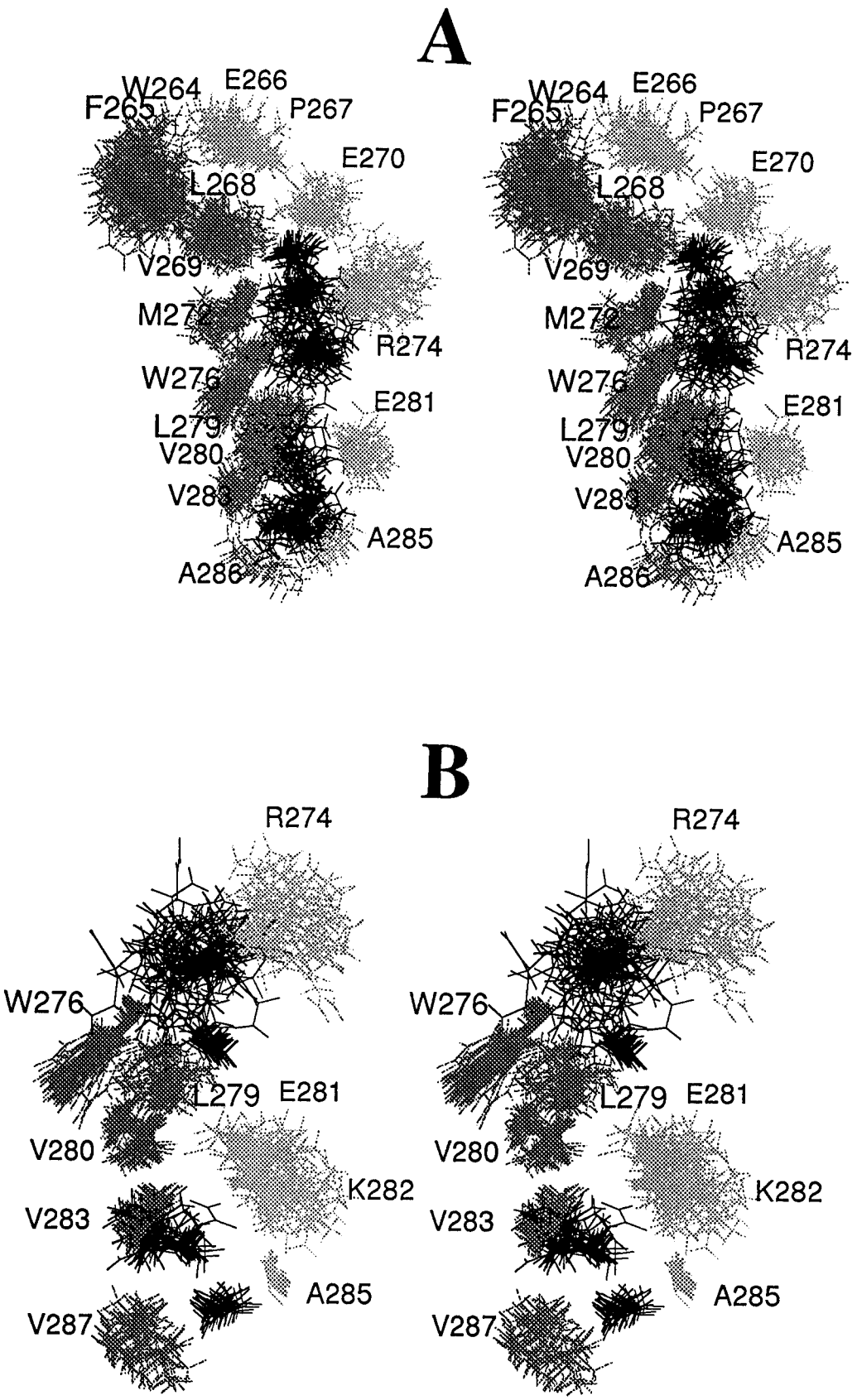

FIGURE 7: Stereoview of the side chains of apoE(263−286) (A) and apoE(267−289) (B) in SDS-d_{25} with backbone atoms omitted for clarity. Hydrophobic side chains are shown in medium gray, hydrophilic side chains in light gray, and interfacial side chains in dark gray. Side chains are selectively labeled. In panel A, interfacial side chains from top to bottom are D271, Q273, Q275, A277, K282, and Q284. In panel B, side chains of residues 267−273 and 288−289 are not shown due to fraying.

observed with apoA-I(166−185) in the presence of SDS wherein the terminal Y166 residue orients toward the hydrophobic face due to interaction with SDS (Wang et al., 1996). The WFLV hydrophobic cluster in apoE(263−286) would explain its strong binding to DMPC, whereas apoE-(267−286), lacking such a cluster, does not bind to DMPC

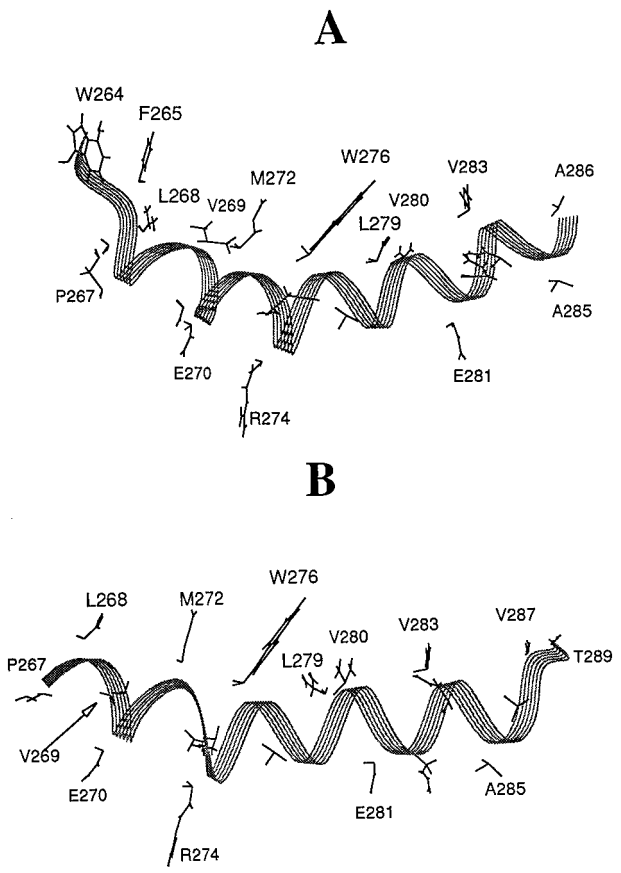

FIGURE 8: Side view of the average structures of apoE(263−286) (A) and apoE(267−289) (B) in SDS-d_{25} with backbone atoms replaced by ribbons. Hydrophobic side chains are clustered on the same side forming the hydrophobic face, whereas hydrophilic side chains are randomly distributed on the opposite side. Interfacial side chains D271, Q273, Q275, A277, K282, and Q284 are not labeled for clarity. Excursions of longer side chains such as R274 and K282 were defined by a cone with the average orientatation corresponding to the axis of the cone.

at all (Sparrow et al., 1992). The W276 side chain in both apoE peptides has very restricted motion as a result of intercalation into the micelle interior. We have observed similar intercalation of aromatic side chains into the hydrophobic core with other apolipoprotein fragments (Rozek et al., 1995) and the LCAT-activating peptide LAP-20 in both SDS and DPC (Buchko et al., 1996), so the effect appears to be general. We therefore propose that aromatic side chains are especially important in anchoring apolipoprotein fragments to lipid complexes.

Biological Implications. The strong lipid binding by the amphipathic sequence containing residues 263−286 has been elucidated by Sparrow et al. (1992), using synthetic peptides, and subsequently confirmed by Westerlund and Weisgraber (1993) using truncation mutagenesis studies, thus identifying an important phospholipid-binding region of apoE. In the present work, we have elucidated the detailed structure of this region by NMR, further confirming the amphipathic helical nature of one of the principal lipid-binding sequences of apoE.

All of the human plasma apolipoproteins contain such strong amphipathic helical binding domains at or near their carboxyl termini. The significance of these amphipathic helices is most probably for the rapid association of the apoprotein with phospholipid. Indeed, Holvoet et al. (1995) have recently shown, using deletion mutagenesis of apoA-I, that the rate of binding with DMPC is reduced 10-fold in a mutant lacking residues 190−243, a region shown by Sparrow and Gotto (1982) to bind to DMPC. The LCAT activation results in that investigation also would indicate that these regions may be important in the organization of the lipids in lipoproteins. These hydrophobic amphipathic helices may also be important in initiating the secondary and tertiary structure of the apoprotein as they associate with lipoprotein particles or assemble new particles. Strong lipid-binding domains probably control the release and rapid capture of the apoprotein during lipolysis or during transfer between lipoprotein particles in circulation. They may also control the number of apoproteins on lipoprotein particles and may, thereby, influence the ultimate size of the lipoprotein and direct its metabolism.

ACKNOWLEDGMENT

We thank R. Storjohann for software and A. Rozek, Drs. R. B. Cornell, G. W. Buchko, and S. J. Dunne, all of Simon Fraser University, for useful discussions.

SUPPORTING INFORMATION AVAILABLE

Two tables showing proton chemical shifts of apoE(263−286), pH 4.8, and apoE(267−289), pH 6.0, in SDS-d_{25} micelles at 37 °C ($H_2O/^2H_2O$ 9:1), peptide/SDS molar ratio of 1:90 and calculated H^α secondary shifts (Wishart et al., 1991) (4 pages). Ordering information is given on any current masthead page.

REFERENCES

Bairaktari, E., Mierke, D. F., Mammi, S., & Peggion, E. (1990) *Biochemistry 29*, 10090−10096.
Barlow, D. J., & Thornton, J. M. (1988) *J. Mol. Biol. 201*, 610−619.
Basu, G., Bagchi, K., & Kuki, A. (1991) *Biopolymers 31*, 1763−1774.
Bax, A., & Davis, D. G. (1985) *J. Magn. Reson. 65*, 355−360.
Berndt, K. D., Güntert, P., & Wüthrich, K. (1996) *Proteins: Struct., Funct., Genet. 24*, 304−313.
Brasseur, R., Lins, L., Vanloo, B., Ruysschaert, J.-M., & Rosseneu, M. (1992) *Proteins: Struct., Funct., Genet. 13*, 246−257.
Braunschweiler, L., & Ernst, R. R. (1983) *J. Magn. Reson. 53*, 521−528.
Brown, L. R., & Wüthrich, K. (1981) *Biochim. Biophys. Acta 647*, 95−111.
Buchko, G. W., Rozek, A., Zhong, Q., & Cushley, R. J. (1995) *Pept. Res. 8*, 86−94.
Buchko, G. W., Treleaven, W. D., Dunne, S. J., Tracey, A. S., & Cushley, R. J. (1996) *J. Biol. Chem. 271*, 3039−3045.
Burley, S. K., & Petsko, G. A. (1985) *Science 229*, 23−28.
Chupin, V., Killian, J. A., Breg, J., De Jongh, H. H. J., Boelens, R., Kaptein, R., & De Kruijff, B. (1995) *Biochemistry 34*, 11617−11624.
Dyson, H. J., Rance, M., Houghten, R. A., Wright, P. E., & Lerner, R. A. (1988) *J. Mol. Biol. 201*, 201−217.
Dyson, H. J., Merutka, G., Waltho, J. P., Lerner, R. A., & Wright, P. E. (1992) *J. Mol. Biol. 226*, 795−817.
Gronenborn, A. M., & Clore, G. M. (1995) *CRC Crit. Rev. Biochem. Mol. Biol. 30*, 351−385.
Havel, T. F. (1991) *Prog. Biophys. Mol. Biol. 56*, 43−78.
Henry, G. D., & Sykes, B. D. (1994) *Methods Enzymol. 239*, 515−535.
Holvoet, P., Zhao, Z., Vanloo, B., Vos, R., Deridder, E., Dhoest, A., Taveirne, J., Brouwers, E., Demarsin, E., Engelborghs, Y., Rosseneu, M., Collen, D., & Brasseur R. (1995) *Biochemistry, 34*, 13334−13342.
Holzwarth, G. M., & Doty, P. (1965) *J. Am. Chem. Soc. 87*, 218−228.

Inagaki, F., Shimada, I., Kawaguchi, K., Hirano, M., Terasawa, I., Ikura, T., & Go, N. (1989) *Biochemistry 28*, 5985−5991.
Innerarity, T. L., Pitas, R. E., & Mahley, R. W. (1979) *J. Biol. Chem. 254*, 4186−4190.
Innerarity, T. L., Friedlander, E. J., Rall, R. L., Jr., Weisgraber, K. H., & Mahley, R. W. (1983) *J. Biol. Chem. 258*, 12341−12347.
Jeener, J., Meier, B. H., Bachmann, P., & Ernst, R. R. (1979) *J. Chem. Phys. 71*, 4546−4553.
Johnson, B. A., Stevens, S. P., & Williamson, J. M. (1994) *Biochemistry 33*, 15061−15070.
Johnson, C. E., & Bovey, F. A. (1958) *J. Chem. Phys. 29*, 1012−1014.
Lauterwein, J., Bosch, C., Brown, L. R., & Wüthrich, K. (1979) *Biochim. Biophys. Acta 556*, 244−264.
Lowry, H. O., Rosebrough, N. J., Farr, A. L., & Randall, R. J. (1951) *J. Biol. Chem. 193*, 265−275.
Mahley, R. W., & Innerarity, T. L. (1983) *Biochim. Biophys. Acta 737*, 197−222.
McDonnell, P. A., & Opella, S. J. (1993) *J. Magn. Reson. B102*, 102−125.
Mishra, V. K., Palgunachari, M. N., Segrest, J. P., & Anantharamaiah, G. M. (1994) *J. Biol. Chem. 269*, 7185−7195.
Nolte, R. T., & Atkinson, D. (1992) *Biophys. J. 63*, 1221−1239.
Pauw, M. D., Vanloo, B., Weisgraber, K., & Rosseneu, M. (1995) *Biochemistry 34*, 10953−10960.
Perczel, A., Park, K., & Fasman, G. D. (1992) *Anal. Biochem. 203*, 83−93.
Pierens, G. K., Buchko, G. W., Wang, G., Treleaven, W. D., Rozek, A., & Cushley, R. J. (1995) *Bull. Magn. Reson. 17*, 292−293.
Piotto, M., Saudek, V., & Sklenár, V. (1992) *J. Biomol. NMR 2*, 661−665.
Raj, P. A., Soni, S.-D., & Levine, M. J. (1994) *J. Biol. Chem. 269*, 9610−9619.
Rall, S. C., Jr., Weisgraber, K. H., & Mahley, R. W. (1982) *J. Biol. Chem. 257*, 4171−4178.
Rance, M., Sørensen, O. W., Bodenhausen, G., Wagner, G. Enrst, R. R., & Wüthrich, K. (1983*) Biochem. Biophys. Res. Commun. 117*, 479−485.
Redfield, A. G., & Kuntz, S. D. (1975) *J. Magn. Reson. 19*, 250−254.
Rizo, J., Blanco, F. J., Kobe, B., Bruch, M. D., & Gierasch, L. M. (1993) *Biochemistry 32*, 4881−4894.
Rozek, A., Buchko, G. W., & Cushley, R. J. (1995) *Biochemistry 34*, 7401−7408.
Segrest, J. P., De Loof, H., Dohlman, J. G., Brouillette, C. G., & Anantharamaiah, G. M. (1990) *Proteins: Struct., Funct., Genet. 8*, 103−117.
Segrest, J. P., Graber, D. W., Brouillette, C. G., Harvey, S. C., & Anantharamaiah, G. M. (1994) *Adv. Protein Chem. 45*, 303−369.
Serrando, L., Bycroft, M., & Fersht, A. R. (1991) *J. Mol. Biol. 218*, 465−475.
Shoemaker, K. R., Kim, P. S., York, E. J., Stewart, J. M., & Baldwin, R. L. (1987) *Nature 326*, 563−567.
Sklenár, V., Piotto, M., Leppik, R., & Saudek, V. (1993) *J. Magn. Reson. A102*, 241−245.
Sparrow, J. T., & Gotto, A. M., Jr. (1982) *CRC Crit. Rev. Biochem. 13*, 87−107.
Sparrow, J. T., Sparrow, D. A., Fernando, G., Culwell, A. R., Kovar, M., & Gotto, A. M., Jr. (1992) *Biochemistry 31*, 1065−1068.
Wang, G., Treleaven, W. D., & Cushley, R. J. (1996) *Biochim. Biophys. Acta* (in press).
Weisgraber, K. H. (1994) *Adv. Protein Chem. 45*, 249−302.
Westerlund, J. A., & Weisgraber, K. H. (1993) *J. Biol. Chem. 268*, 15745−15750.
Wetterau, J. R., Aggerbeck, L. P., Rall, S. C., Jr., & Weisgraber, K. H. (1988) *J. Biol. Chem. 263*, 6240−6248.
Wilson, C., Wardell, M. R., Weisgraber, K. H., Mahley, R. W., & Agard, D. A. (1991) *Science 252*, 1817−1822.
Wishart, D. S., Sykes, B. D., & Richards, F. M. (1991) *J. Mol. Biol. 222*, 311−333.
Wishart, D. S., Sykes, B. D., & Richards, F. M. (1992) *Biochemistry 31*, 1647−1651.
Woody, R. W. (1995) *Methods Enzymol. 246*, 34−71.
Wüthrich, K. (1986) *NMR of Proteins and Nucleic Acids*, Wiley, New York.
Wüthrich, K., Billeter, M., & Braun, W. (1984) *J. Mol. Biol. 180*, 715−740.
Yee, A. A., Babiuk, R., & O'Neil, J. D. J. (1995) *Biopolymers 36*, 781−792.
Yuan, T., Mietzner, T. A., Montelaro, R. C., & Vogel, H. J. (1995) *Biochemistry 34*, 10690−10696.
Yun, R. H., Anderson, A., & Hermans, J. (1991) *Proteins: Struct., Funct., Genet. 10*, 219−228.
Zhong, Q., Clark-Lewis, I., & Cushley, R. J. (1994) *Pept. Res. 7*, 99−106.

BI960934T